

# RSC Advances



This is an *Accepted Manuscript*, which has been through the Royal Society of Chemistry peer review process and has been accepted for publication.

*Accepted Manuscripts* are published online shortly after acceptance, before technical editing, formatting and proof reading. Using this free service, authors can make their results available to the community, in citable form, before we publish the edited article. This *Accepted Manuscript* will be replaced by the edited, formatted and paginated article as soon as this is available.

You can find more information about *Accepted Manuscripts* in the [Information for Authors](#).

Please note that technical editing may introduce minor changes to the text and/or graphics, which may alter content. The journal's standard [Terms & Conditions](#) and the [Ethical guidelines](#) still apply. In no event shall the Royal Society of Chemistry be held responsible for any errors or omissions in this *Accepted Manuscript* or any consequences arising from the use of any information it contains.

## Efficient Absorption of Ammonia with Hydroxyl-functionalized Ionic Liquids

Zhijie Li,<sup>ab</sup> Xiangping Zhang,<sup>\*a</sup> Haifeng Dong,<sup>a</sup> Xiaochun Zhang,<sup>a</sup> Hongshuai Gao,<sup>a</sup> Suojiang Zhang,<sup>\*a</sup> Jianwei Li<sup>b</sup> and Congmin Wang<sup>c</sup>

<sup>a</sup> Beijing Key Laboratory of Ionic Liquids Clean Process, State Key Laboratory of Multiphase Complex Systems, Institute of Process Engineering, Chinese Academy of Sciences, Beijing, 100190, China

<sup>b</sup> State Key Laboratory of Chemical Resource Engineering, Beijing University of Chemical Technology, Beijing, 100029, China

<sup>c</sup> Department of Chemistry, Zhejiang University, Hangzhou, 310027, China

### ABSTRACT:

Ammonia (NH<sub>3</sub>) emitted from ammonia synthesis process is a kind of waste chemical resource and a major environmental pollutant. The traditional water scrubbing method suffers from high energy consumption due to the concentrated NH<sub>3</sub> from aqueous ammonia. Therefore, it is desirable to develop novel absorbents for the efficient, reversible and environment-friendly recovery of NH<sub>3</sub>. In this paper, a series of hydroxyl-functionalized imidazolium ILs ([EtOHmim]X, X=[NTf<sub>2</sub>], [PF<sub>6</sub>], [BF<sub>4</sub>], [DCA], [SCN] and [NO<sub>3</sub>]) were designed and prepared. Their physical properties and NH<sub>3</sub> absorption capacities under different temperatures and pressures were systematically investigated. The effects of hydroxyl cation, anionic structures, pressure and temperature on absorption performance were sufficiently studied. In addition, the absorption mechanism was detailedly investigated by spectral analysis and quantum chemistry calculations. Compared with conventional IL [Emim]X, a higher absorption capacity was achieved by introducing the hydroxyl group on the imidazolium cation. The mechanism results showed the fascinating absorption performance of the task-specific ILs was attributed to the stronger hydrogen bonding interaction between NH<sub>3</sub> and the H atom of hydroxyl group. Considering the excellent absorption performance, high thermal stability, and super reversibility, this type of IL provides great improvement over conventional IL and shows their enormous potentials in NH<sub>3</sub> recovery.

**Keywords:** hydroxyl-functionalized, ionic liquids, ammonia, absorption

## 1. INTRODUCTION

As a typical environmental pollutant, the increasing of ammonia ( $\text{NH}_3$ ) emission is leading to different environmental problems including eutrophication of ecosystem and the formation of fine particulate matter<sup>1</sup> and seriously threatens human health. Meanwhile,  $\text{NH}_3$  is one of the important chemical raw materials and widely applied in producing nitric acid, nitrogenous fertilizer and so on. Therefore, removal and recovery of  $\text{NH}_3$  is of great significance. Up to now, water scrubbing is the most common method due to its high  $\text{NH}_3$  absorption capacity. However, this method suffers from several inherent drawbacks such as high energy consumption, large amounts of waste water and difficult reclamation of  $\text{NH}_3$ . Hence, it is desirable to develop environment-friendly, recyclable absorbents for efficient  $\text{NH}_3$  absorption.

It is increasingly recognized that ionic liquids (ILs) are promising absorbents because of their special properties such as negligible vapor pressure, wide liquid temperature range, high thermal stability<sup>2</sup> and adjustability<sup>3</sup> and have been paid great attentions on separation of  $\text{CO}_2$ <sup>4-11</sup>,  $\text{SO}_2$ <sup>12-19</sup> and  $\text{H}_2\text{S}$ <sup>6, 20-23</sup>. On the contrast, the reports on  $\text{NH}_3$  absorption by ionic liquids are scarce. In fact, the results reported have shown that ionic liquids have great potentials for  $\text{NH}_3$  absorption. Yokozeki *et al.*<sup>24, 25</sup> demonstrated the conventional ionic liquids such as [Bmim][PF<sub>6</sub>], [Hmim][Cl] had high  $\text{NH}_3$  absorption performance and the anion had little effect on  $\text{NH}_3$  solubility. Li *et al.*<sup>26</sup> reported  $\text{NH}_3$  solubility increased when the length of cation's alkyl increased. Shi *et al.*<sup>27</sup> testified the cation played the leading role in determining  $\text{NH}_3$  solubility and they found a strong hydrogen bonding could be formed between  $\text{NH}_3$  molecule and the ring H atom of the [Emim] cation by molecular simulation.

Although great efforts had been made to improve the  $\text{NH}_3$  absorption, the solubility of  $\text{NH}_3$  in these conventional ILs was relatively low. What is more, the research on the mechanism of IL- $\text{NH}_3$  system was very scanty and not comprehensive. Shi *et al.*<sup>27</sup> investigated the  $\text{NH}_3$  absorption mechanism just by molecular simulation. As reported, hydrogen bonding interaction between IL and  $\text{NH}_3$  was beneficial to enhance solubility<sup>28</sup>, thus in this work, hydroxyl, as the hydrogen bonding donor group, was introduced into the imidazolium cation for further improving the absorption.  $\text{NH}_3$  absorption capacities of these hydroxyl-functionalized ILs at different temperatures and pressures were systematically investigated. Furthermore, the absorption mechanism was systematically and deeply explored by experimental spectra analysis and quantum chemistry calculations.

## 2. EXPERIMENTAL SECTION

**2.1. Materials.**  $\text{NH}_3$  (99.999%) was supplied by Beijing Beiwen Gas Factory. 1-Methylimidazole (99.0%),  $\text{NaBF}_4$  (98.0%),  $\text{LiNTf}_2$  (98.5%) and  $\text{NaSCN}$  (98.5%) were

purchased from Sinopharm Chemical Reagent Co., Ltd. 2-Chloroethanol (99.0%) was purchased from Xiya Chemical Co., Ltd.  $\text{KPF}_6$  (98.0%) and  $\text{NaNO}_3$  (99.0%) were purchased from Beijing Chemical Works Co., Ltd. All the chemicals above were used without further purification. 1-ethyl-3-methylimidazolium chloride was obtained from Linzhou Keneng Materials Technology Co., Ltd. 1-2-(hydroxyethyl)-3-methylimidazolium salt  $[\text{EtOHmim}]\text{X}$  and 1-ethyl-3-methylimidazolium salt  $[\text{Emim}]\text{X}$  were synthesized in our laboratory.

**2.2. Synthesis of Ionic Liquids.**  $[\text{EtOHmim}][\text{NTf}_2]$  was synthesized by the method shown in Scheme S1 (seeing supplementary information) according to the literature<sup>29</sup>. Preparation of  $[\text{EtOHmim}][\text{Cl}]$ : 1-Methylimidazole (41.00 g, 0.5 mol) was put in a round-bottom flask (250 mL) and 2-Chloroethanol (48.31 g, 0.6 mol) was added slowly. The mixture was stirred for 24 hours at 353.15 K. Then the product was washed several times with ethyl acetate. The  $[\text{EtOHmim}][\text{Cl}]$  white solid was obtained after filtration and vacuum drying for 48 hours at 343.15 K. Preparation of  $[\text{EtOHmim}][\text{NTf}_2]$ :  $[\text{EtOHmim}][\text{Cl}]$  (16.252 g, 0.1 mol) and  $\text{LiNTf}_2$  (28.69 g, 0.1 mol) were mixed and some water was added as solvent. Then the mixture was stirred for 24 hours at ambient temperature. By separating the mixture, the supernate was removed and ionic liquid was washed by deionized water for several times until there was no sediment formed when  $\text{AgNO}_3$  was added in water. At last, high-purity  $[\text{EtOHmim}][\text{NTf}_2]$  was obtained after rotary evaporation and vacuum drying at 373.15 K for 64 hours. The synthesis methods of other ILs  $[\text{EtOHmim}]\text{X}$  ( $\text{X} = [\text{PF}_6]^-$ ,  $[\text{BF}_4]^-$ ,  $[\text{DCA}]^-$ ,  $[\text{SCN}]^-$ ,  $[\text{NO}_3]^-$ ) and  $[\text{Emim}]\text{X}$  ( $\text{X} = [\text{NTf}_2]^-$ ,  $[\text{BF}_4]^-$ ,  $[\text{NO}_3]^-$ ) were similar to that of  $[\text{EtOHmim}][\text{NTf}_2]$  except the solvent was replaced by acetone. The different structures of  $[\text{EtOHmim}]^+$  cation and  $[\text{Emim}]^+$  cation were presented in Figure 1.

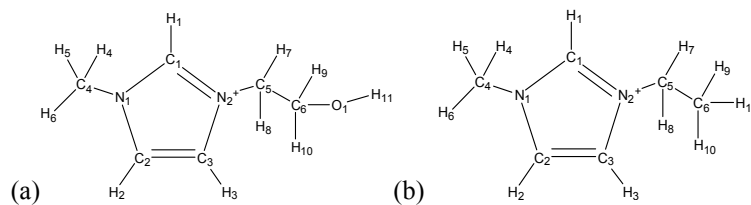


**Figure 1.** Schematics of  $[\text{EtOHmim}]^+$  (a) and  $[\text{Emim}]^+$  (b), with atom labels.

**2.3. Characterization and Physical Properties.**  $^1\text{H}$  NMR and  $^{13}\text{C}$  NMR spectra were recorded on a Bruker spectrometer (600 Hz) in deuterated dimethyl sulfoxide ( $\text{DMSO}-d_6$ ) with tetramethylsilane as the internal standard. The NMR data of ILs were presented in supplementary information. FT-IR spectra were obtained in the range of  $400\text{--}4000\text{ cm}^{-1}$  on a Thermo Nicolet 380 spectrometer. The water contents of the ILs were measured by Karl Fisher coulometers C20 and had been reduced less than 400 ppm. The chlorine contents were tested by ioniza chlorine andlyzer (Leici PXSJ-226). The densities of ionic liquids were measured by a density meter (Anton Paar DMA 5000) with an accuracy of  $\pm 0.000\ 005\text{ g cm}^{-3}$ . The viscosities were measured

by an automated micro viscometer (Anton Paar AMVn). The thermal decomposition temperatures were tested by TGA (Q5000 V3.15 Build 263) from room temperature to 773.15 K with a heating rate of 10 K/min under N<sub>2</sub> atmosphere. The glass transition temperatures were measured on a Mettler Toledo DSC1 between 123.15 and 298.15 K at a heating rate of 10 K/min under N<sub>2</sub> atmosphere.

**2.4. Apparatus and Procedures.** NH<sub>3</sub> solubility was measured by the gas-liquid equilibrium apparatus (shown in Figure 2) which was similar to that in our previous work<sup>17,30</sup>. In a typical experiment, the temperature was fixed by a thermostatic water bath with an uncertainty of ± 0.1 K and the pressure was measured by pressure transmitters with an accuracy of 0.0001 kPa. About 5.0 g IL was placed into the absorption vessel (30 mL), then the gas in absorption vessel was removed by vacuum pump. The NH<sub>3</sub> in storage tank (500 mL) was charged into the absorption vessel slowly through the valve (b<sub>2</sub>). Then the magnetic stirrer was opened to enhance the dissolution. It is supposed the equilibrium is reached after the pressure keeps unchanged for 30 min. The solubility of NH<sub>3</sub> was calculated by Peng-Robinson (*P-R*) equation (1) through the pressure variation in storage tank and absorption vessel:

$$p = \frac{RT}{V_m - b} - \frac{a}{V_m(V_m + b) + b(V_m - b)} \quad (1)$$

$$a = a_c \alpha \quad (1.1)$$

$$a_c = 0.457235 \frac{(RT_c)^2}{p_c} \quad (1.2)$$

$$b = 0.077796 \frac{RT_c}{p_c} \quad (1.3)$$

$$\alpha^{0.5} = 1 + (0.37464 + 1.54226\omega - 0.26992\omega^2)(1 - T_r^{0.5}) \quad (1.4)$$

$$T_r = \frac{T}{T_c} \quad (1.5)$$

$$n_{NH_3} = \Delta \left( \frac{V_S}{V_{m,S}} \right) - \left( \frac{V_A - V_{IL}}{V_{m,A}} \right) \quad (2)$$

$$x_{NH_3} = \frac{n_{NH_3}}{n_{NH_3} + n_{IL}} \quad (3)$$

Where  $p$ ,  $V_m$  and  $T$  are denoted to pressure, molar volume and temperature, respectively.  $R$  is the gas constant and  $a$ ,  $b$ ,  $a_c$ ,  $\alpha$  are the parameters of the cubic equation.  $T_c$  is the critical temperature,  $p_c$  is the critical pressure and  $T_r$  is relative temperature.  $n_{NH_3}$  is the amount of

$\text{NH}_3$  absorbed and  $n_{IL}$  is the amount of ionic liquid.  $V_S$ ,  $V_A$  and  $V_{IL}$  represent the volumes of storage tank, absorption vessel and ionic liquid, respectively.  $V_{m,S}$  and  $V_{m,A}$  are the molar volume of storage tank and absorption vessel.  $x_{\text{NH}_3}$  represents the mole fraction of  $\text{NH}_3$  absorbed.

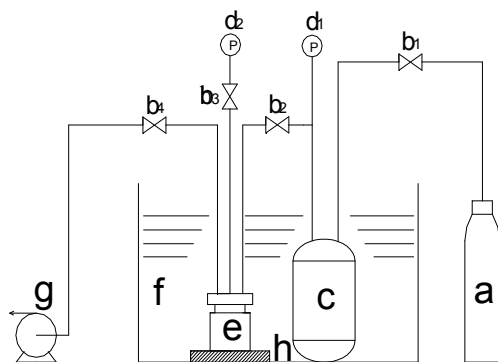


**Figure 2.** Schematic diagram of  $\text{NH}_3$  absorption apparatus.

a,  $\text{NH}_3$  cylinder;  $b_1$ ~ $b_4$ , valve; c, storage tank;  $d_1$ ~ $d_2$ , pressure sensor; e, absorption vessel; f, thermostatic bath; g, vacuum pump; h, magnetic stirrer.

**2.5. Thermodynamic Analysis.** Henry's constant ( $k_H$ ) is an important parameter to present the absorption behavior of  $\text{NH}_3$  in ILs. The Henry's constants of  $\text{NH}_3$  absorbed in ionic liquids at different temperatures could be obtained by the following equation (4) and the fugacity coefficient ( $\varphi$ ) was calculated according to the  $P$ - $R$  equation. Subsequently, the changes of standard Gibbs free energy ( $\Delta_{sol}G^\theta$ ), standard enthalpy ( $\Delta_{sol}H^\theta$ ) and standard entropy ( $\Delta_{sol}S^\theta$ ) could be estimated by the following equations (6), (7) and (8).

$$k_H(T) = \lim_{P \rightarrow 0} \left[ \frac{f_1(T, p)}{x_1} \right] = \frac{p^{eq} \varphi_1(T, p)}{x_1} \quad (4)$$

$$\ln \varphi = \frac{pV}{RT} - 1 - \ln \frac{p(V-b)}{RT} - \frac{\alpha}{2^{1.5} bRT} \ln \frac{V + (\sqrt{2} + 1)b}{V - (\sqrt{2} - 1)b} \quad (5)$$

$$\Delta_{sol}G^\theta = RT \ln(k_H / p^\theta) \quad (6)$$

$$\Delta_{sol}H^\theta = -RT^2 \frac{\partial \ln(k_H / p^\theta)}{\partial T} \quad (7)$$

$$\Delta_{sol}S^\theta = \frac{\Delta_{sol}H^\theta - \Delta_{sol}G^\theta}{T} \quad (8)$$

Where  $f_1(T, p)$  represents the fugacity of  $\text{NH}_3$  and  $\varphi_1(T, p)$  is the fugacity coefficient of  $\text{NH}_3$  solute in the gas phase.  $p^{eq}$  is the equilibrium partial pressure of  $\text{NH}_3$  and  $p^\theta$  represents the standard pressure.

### 3. RESULTS AND DISCUSSION

**3.1. Physical Properties of ILs.** Density and viscosity of IL were fundamental properties for gas separation process, hence these properties were measured at different temperatures from 298.15 K to 343.15 K. Figure 3 shows the densities of the functionalized ILs decrease linearly with the increasing of temperature and they fall in the range from 1.15 to 1.58  $\text{g cm}^{-3}$ . It can be found the densities are greatly affected by the different anions and [EtOHmim][DCA] shows the lowest density.

Figure 4 shows the viscosities of the functionalized ILs with different anions range from 19.10 to 609.98 mPa.s and decrease in an exponential manner with the increasing of temperature, which is in agreement with the other imidazolium ILs<sup>31</sup>. Viscosity activation energy ( $E_a$ ) of IL is estimated by a fitting of the measured viscosity to Arrhenius expression<sup>32</sup> using the following equation:

$$\eta = \eta_\infty \exp(-E_a / RT) \quad (9)$$

In this equation,  $\eta$  is the viscosity at any temperature and  $\eta_\infty$  is the apparent viscosity at infinite temperature. The values of  $E_a$  for [EtOHmim]X shown in Table S1 and they range from 31 to 45  $\text{kJ mol}^{-1}$ . Generally, the larger value will indicate the higher viscosity. The calculated viscosity activation energies of the task-specific ILs are larger than those of the typical solutions ( $E_{a_{\text{water}}}=17.0 \text{ kJ mol}^{-1}$ ,  $E_{a_{\text{benzene}}}=10.4 \text{ kJ mol}^{-1}$ , and  $E_{a_{\text{acetone}}}=7.1 \text{ kJ mol}^{-1}$ )<sup>33</sup>. Although [EtOHmim][DCA] shows the lowest viscosity, the introducing of hydroxyl group results in the larger viscosity than that of [Emim][DCA] (18.4  $\text{kJ mol}^{-1}$ ), which indicates that cations also influence the viscosity.

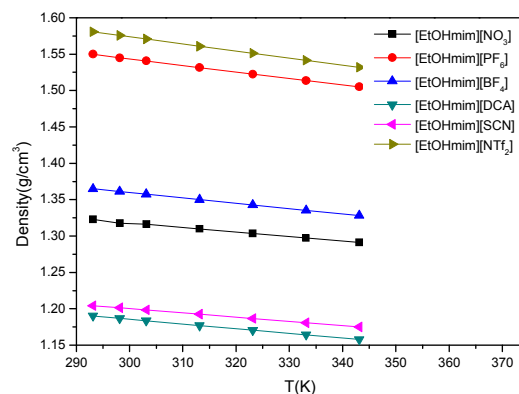


**Figure 3.** Densities of task-specific ILs at different temperatures.

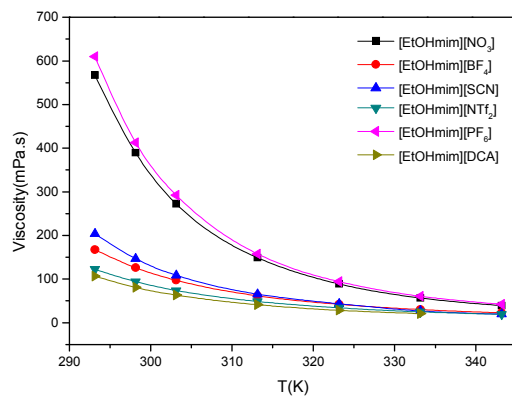


**Figure 4.** Viscosities of task-specific ILs at different temperatures.

In addition, thermal stability of IL is also very significant for gas separation, because high thermal stability is beneficial for reversible absorption and desorption. The TGA curves are shown in Figure S2 and the results of DSC and TGA are summarized in Table 1. The thermal decomposition temperatures ( $T_d$ ) of the six functionalized ILs are all above 500 K and [EtOHmim][NTf<sub>2</sub>] shows the highest decomposition temperature. Pablo's group reported the  $T_d$  of [Emim][SCN] was 538.6 K<sup>34</sup>, which was similar to that of [EtOHmim][SCN]. It shows the introducing of hydroxyl is almost no influence on the thermal stability.

**Table 1.** The melting points ( $T_m$ ), glass transition temperatures ( $T_g$ ) and the thermal decomposition temperatures ( $T_d$ ) of the functionalized ILs.

[EtOHmim]X	$T_m$ (K)	$T_g$ (K)	$T_d$ (K)
[NTf <sub>2</sub> ]	-	190.02	643.75
[PF <sub>6</sub> ]	308.32	187.67	564.11
[BF <sub>4</sub> ]	-	187.98	542.81
[DCA]	-	185.28	507.18
[SCN]	286.32	185.64	543.91



[NO <sub>3</sub> ]	281.32	183.35	546.42
--------------------	--------	--------	--------

**3.2. NH<sub>3</sub> Absorption Performance of [EtOHmim]X.** First, NH<sub>3</sub> absorption capacity of [Bmim][BF<sub>4</sub>] was investigated at 298.15 K and compared with values reported from the available literatures in order to validate the reliability of data in this work. Figure 5 shows the solubility is similar to that in literatures<sup>25,26</sup>, which indicates that the experiment apparatus is reliable and the data is credible. Then, a series of vapor liquid equilibrium measurements were performed at pressures from 0 to 0.6 MPa (A) and temperatures from 298.15 to 343.15 K. The solubility data of pressure-temperature-composition (*p-T-x*) of the task-specific ILs are presented in supplementary information Table S2.

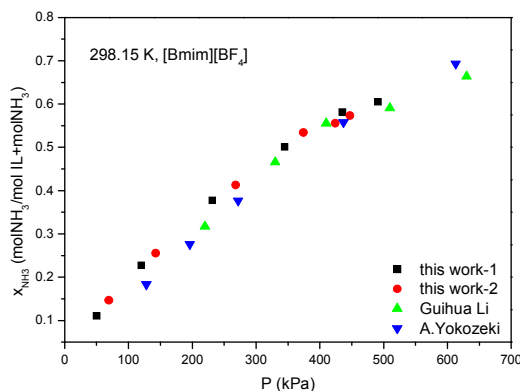


**Figure 5.** NH<sub>3</sub> absorption capacity of [Bmim][BF<sub>4</sub>] in this work and the literatures<sup>25,26</sup> at 298.15 K.

**3.2.1 Effect of Hydroxyl Group cation.** To assess the effect of hydroxyl group cation on NH<sub>3</sub> solubility, the absorption capacity of functionalized ILs [EtOHmim]X were compared with that of conventional ILs [Emim]X at 333.15 K. The results show that the former captures higher amount of NH<sub>3</sub>. Figure 6 shows that when the anion is same, an obvious increase of solubility is found in [EtOHmim]X. For example, At 102.7 kPa, the solubility of [EtOHmim][BF<sub>4</sub>] is 0.27 in mole fraction, and at 547.0 kPa, the mole fraction is 0.56. For [Emim][BF<sub>4</sub>], the solubility at 103.1 kPa is 0.10 and at 548.2 kPa the mole fraction is 0.40. It suggests that the absorption capacities of imidazolium ILs are distinctly enhanced due to the introducing of hydroxyl group. A possible explanation is that hydrogen bonding interaction brings about the improved absorption performance. The acid hydroxyl, regarded as the hydrogen bonding donor group, could form stronger hydrogen bonding with the N atom of NH<sub>3</sub> than the conventional [Emim]X. In addition, because the viscosities of [EtOHmim]X are slightly larger than [Emim]X due to the introducing of hydroxyl group, the equilibrium time for NH<sub>3</sub> absorption in [EtOHmim][NTf<sub>2</sub>] and [Emim][NTf<sub>2</sub>] have been also measured respectively using the same apparatus. The variations of

pressure with time are shown in Figure S3. We can find the equilibrium time of [EtOHmim][NTf<sub>2</sub>] (about 6 min) is slightly longer than [Emim][NTf<sub>2</sub>] (about 4 min). In conclusion, hydroxyl-functionalized ILs may be more suitable to be the solvents for NH<sub>3</sub> recovery than conventional ILs.

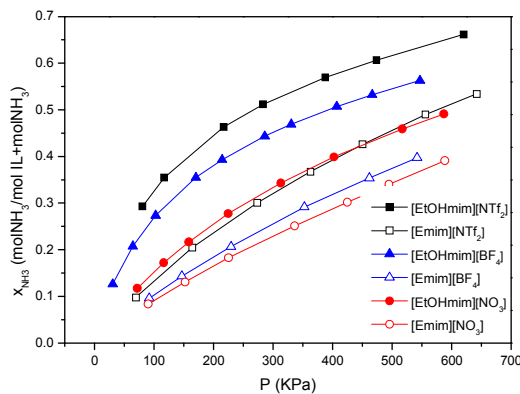


**Figure 6.** Comparison of NH<sub>3</sub> solubilities in [EtOHmim]X and [Emim]X (X = [NTf<sub>2</sub>]<sup>-</sup>, [BF<sub>4</sub>]<sup>-</sup>, [NO<sub>3</sub>]<sup>-</sup>) at 333.15 K.

**3.2.2 Effect of Anions.** With the comparison of NH<sub>3</sub> solubilities in ILs with different anions, it is observed that anions also have an obviously effect on NH<sub>3</sub> absorption. Figure 7 presents the ILs of anions contained fluoride ([NTf<sub>2</sub>]<sup>-</sup>, [PF<sub>6</sub>]<sup>-</sup>, [BF<sub>4</sub>]<sup>-</sup>) have higher solubility than others ([DCA]<sup>-</sup>, [SCN]<sup>-</sup>, [NO<sub>3</sub>]<sup>-</sup>). The absorption capacities of these ILs decrease in the following order: [NTf<sub>2</sub>]<sup>-</sup> > [PF<sub>6</sub>]<sup>-</sup> > [BF<sub>4</sub>]<sup>-</sup> > [SCN]<sup>-</sup> > [NO<sub>3</sub>]<sup>-</sup>. Especially, for [DCA] anion, when the pressure is less than 150 kPa, its absorption capacity is lower than that of [NO<sub>3</sub>]<sup>-</sup>; but when the pressure is between 150 to 400 kPa, its absorption capacity falls in that between [SCN]<sup>-</sup> and [NO<sub>3</sub>]<sup>-</sup>. The similar conclusion can be obtained at other temperatures. The reason for the higher absorption capacities of ILs containing fluoride may be the F atom of the anions can also form hydrogen bonding interaction with the H atom of NH<sub>3</sub><sup>27</sup>. From a molecular perspective, there are three hydrogen bonding donors on NH<sub>3</sub>, four acceptors on [BF<sub>4</sub>]<sup>-</sup>, six acceptors on [PF<sub>6</sub>]<sup>-</sup> and 10 acceptors on [NTf<sub>2</sub>]<sup>-</sup>. Therefore, the relatively stronger hydrogen bonding interaction may be formed between H atom of NH<sub>3</sub> and [NTf<sub>2</sub>]<sup>-</sup> anion, which is consistent with the highest solubility of [EtOHmim][NTf<sub>2</sub>]. Because of the highest absorption capacity of [EtOHmim][NTf<sub>2</sub>], this ionic liquid is investigated as a typical example.

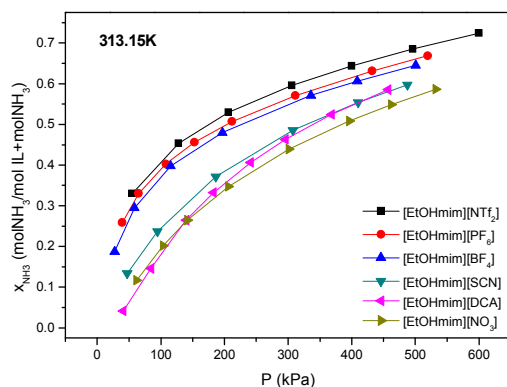


**Figure 7.** The solubilities of  $\text{NH}_3$  in task-specific ILs with different anions at 313.15 K.

**3.2.3 Effects of temperature and pressure.** The effects of temperature and pressure on  $\text{NH}_3$  absorption in  $[\text{EtOHmim}][\text{NTf}_2]$  are displayed in Figure 8. It can be seen that with the increasing of temperature, the absorption capacity of hydroxyl-functionalized ILs dramatically decreases. Besides, the molar fraction of  $\text{NH}_3$  increases continuously with the increasing pressure of  $\text{NH}_3$ . It suggests that low temperature is better for  $\text{NH}_3$  absorption and the desorption can be carried out at high temperature, which is in good agreement with the literature<sup>24</sup>.

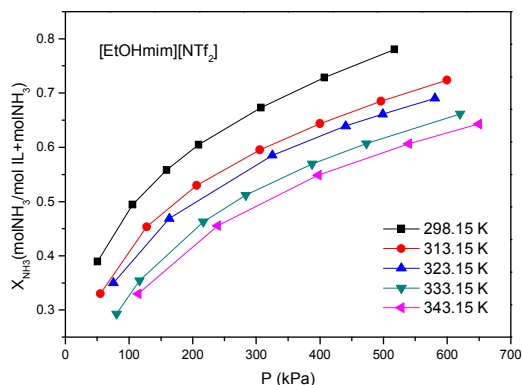


**Figure 8.** The solubilities of  $\text{NH}_3$  in  $[\text{EtOHmim}][\text{NTf}_2]$  at different temperatures.

**3.3. Desorption and Recycling.** Recyclability is another important factor to evaluate an ionic liquid solvent and a key issue for potential industrial application, thus the absorption cycles of  $[\text{EtOHmim}][\text{NTf}_2]$  have been measured at 298.15 K and 100 kPa. First, the solubility was investigated in the fresh IL, then  $\text{NH}_3$ -saturated IL was desorbed under a vacuum of 0.15 kPa for 1 hour at 353.15 K and reused for  $\text{NH}_3$  absorption. The absorption-desorption experiments were performed for five cycles. Figure 9 shows that the solubility keeps almost unchanged after five

cycles. It is revealed that [EtOHmim][NTf<sub>2</sub>] can be reused with almost same capacity, which suggests the functionalized ILs have good recyclability.

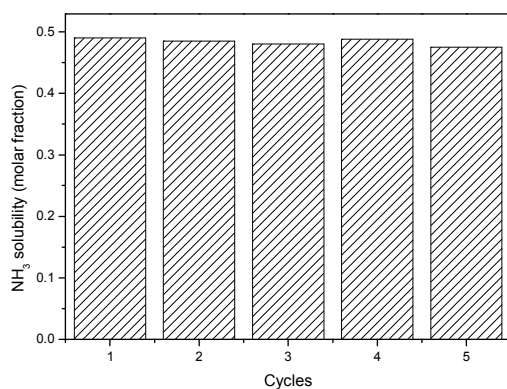


**Figure 9.** Recycling of [EtOHmim][NTf<sub>2</sub>] for NH<sub>3</sub> absorption at 298.15 K and 100 kPa.

**3.4. Thermodynamic Properties of NH<sub>3</sub> in ILs.** Henry's constants were calculated according to the solubility of NH<sub>3</sub>. In Figure 10, with the increasing of temperature, Henry's constants increase for each ionic liquid. The Henry's constants in the ILs containing fluoride are smaller than those of others, which accords with the higher NH<sub>3</sub> absorption capacity of the ILs containing fluoride. Thermodynamic parameters including standard enthalpy, standard Gibbs free energy, and standard entropy were also calculated and the results were presented in Table 2. Solution entropy represents the direction of disorder in the absorption process. Table 2 shows standard Gibbs free energy changes are positive and entropy changes are negative. Namely, at standard pressure, ammonia solution in [EtOHmim]X is a process of entropy decreasing. The value of  $\Delta G$  increases with the increasing of temperature, which means higher temperature is unfavorable for NH<sub>3</sub> absorption. This conclusion is consistent with the experimental results. Solution enthalpy is an important parameter to evaluate the gas-liquid interaction. From Table 2, the enthalpy changes are negative, which indicates the solution at standard pressure is exothermal. And this conclusion corresponds with the ordinary solution rules for most gas. The enthalpy changes increases with the increasing of temperature, it demonstrates the heat release in this solution process decreases with the increasing of temperature. Usually, a higher value of enthalpy signifies a stronger gas-liquid interaction. But for [EtOHmim]X, the order of solubility is not as same as that of enthalpy. For example, the solubility of [EtOHmim][NTf<sub>2</sub>] is significantly higher than [EtOHmim][NO<sub>3</sub>], but the absolute value of enthalpy in [EtOHmim][NO<sub>3</sub>]-NH<sub>3</sub> system is higher than that in [EtOHmim][NTf<sub>2</sub>]-NH<sub>3</sub> system. Therefore, for the ionic liquids with different anions,

not only the interaction between  $\text{NH}_3$  and ILs but also the free volume of anions plays important influence on solubility.

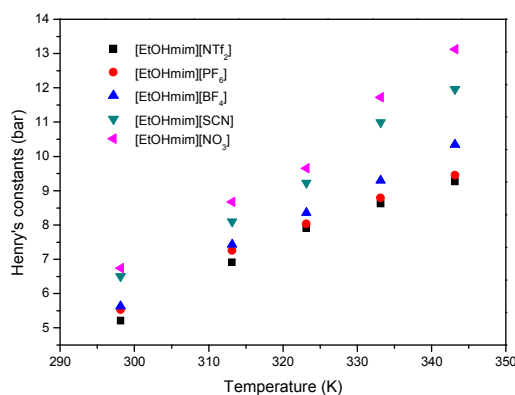


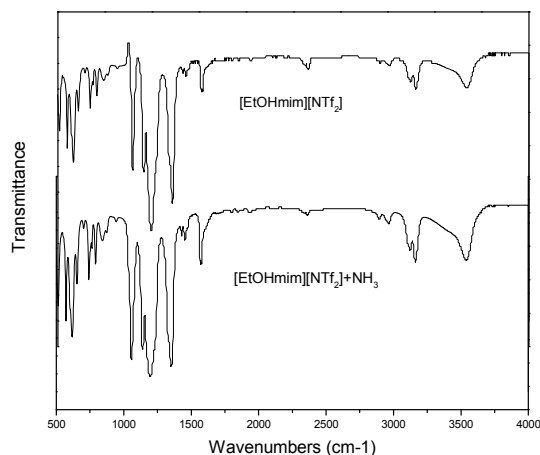
**Figure 10.** Henry's constants of  $\text{NH}_3$  in task-specific ILs versus temperature.

**Table 2.** Thermodynamic parameters of  $\text{NH}_3$  in [EtOHmim]X.

T (K)	[EtOHmim][NTf <sub>2</sub> ]	[EtOHmim][PF <sub>6</sub> ]	[EtOHmim][BF <sub>4</sub> ]	[EtOHmim][SCN]	[EtOHmim][NO <sub>3</sub> ]
$\Delta_{sol}G^{\theta}$ (kJ mol <sup>-1</sup> )					
298.15	4.09	4.24	4.28	4.64	4.73
313.15	5.03	5.16	5.22	5.45	5.62
323.15	5.55	5.60	5.70	5.97	6.09
333.15	5.97	6.02	6.18	6.64	6.82
343.15	6.35	6.41	6.67	7.08	7.34
$\Delta_{sol}H^{\theta}$ (kJ mol <sup>-1</sup> )					
298.15	-9.39	-9.46	-9.83	-10.27	-11.01
313.15	-10.35	-10.44	-10.84	-11.33	-12.15
323.15	-11.03	-11.11	-11.55	-12.07	-12.94
333.15	-11.72	-11.81	-12.27	-12.83	-13.75
343.15	-12.43	-12.53	-13.02	-13.61	-14.59
$\Delta_{sol}S^{\theta}$ (J mol <sup>-1</sup> K <sup>-1</sup> )					
298.15	-45.21	-45.94	-47.33	-50.02	-52.80
313.15	-49.14	-49.80	-51.30	-53.58	-56.75
323.15	-51.31	-51.72	-53.39	-55.82	-58.88
333.15	-53.09	-53.52	-55.38	-58.43	-61.74
343.15	-54.75	-55.20	-57.37	-60.29	-63.91

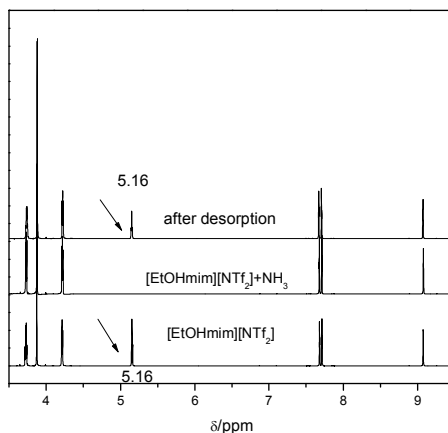
**3.5. Mechanism of  $\text{NH}_3$  Absorption.** The mechanism of  $\text{NH}_3$  absorption is investigated by the comparison of FT-IR and <sup>1</sup>H NMR spectra of [EtOHmim]X before and after  $\text{NH}_3$  absorption. Figure 11 shows that there is no obvious change of FT-IR spectra for [EtOHmim][NTf<sub>2</sub>] before

and after  $\text{NH}_3$  absorption. Furthermore, in-situ FT-IR (shown in Figure S4) is applied to monitor the spectral variation of  $\text{NH}_3$  absorption process for one hour, which also shows no distinct changes. Considering the absorption performance, the easy desorption behavior and no formation of new functional group, a possible explanation is that these novel ionic liquids absorb  $\text{NH}_3$  through hydrogen bonding interaction, such as  $\text{O-H}\cdots\text{N}$ .



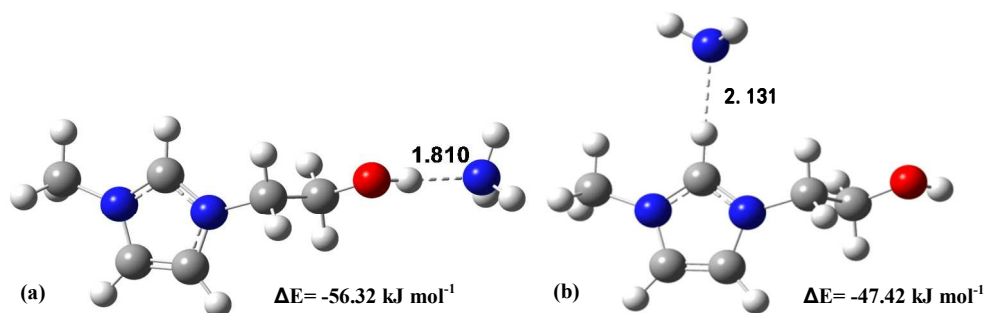
**Figure 11.** FT-IR spectra of  $[\text{EtOHmim}][\text{NTf}_2]$  before and after absorption of  $\text{NH}_3$ .

Meanwhile,  $^1\text{H}$  NMR spectra of  $[\text{EtOHmim}]\text{X}$  before and after absorption of  $\text{NH}_3$  are further studied. First, by comparing the  $^1\text{H}$  NMR spectra of  $[\text{Emim}][\text{NTf}_2]$  and  $[\text{EtOHmim}][\text{NTf}_2]$  (seeing supplementary information Figure S5), the peak at 5.16 ppm is confirmed to be the shift of  $\text{H}_{11}$  atom on the hydroxyl. Figure 12 indicates the peak at 5.16 ppm disappears after  $\text{NH}_3$  absorption and reappears after desorption. And the same phenomenon is also happened in the other functionalized ILs. That shows the shift of the  $\text{H}_{11}$  on hydroxyl may be dramatically affected due to the strong interaction between the electronegative N atom of  $\text{NH}_3$  and  $\text{H}_{11}$  of hydroxyl.



**Figure 12.**  $^1\text{H}$  NMR spectra of  $[\text{EtOHmim}][\text{NTf}_2]$  before and after  $\text{NH}_3$  absorption.

The interaction between hydroxyl-functionalized cation and  $\text{NH}_3$  molecule was further studied by the quantum chemistry calculations at the B3LYP/6-311++G\*\* level with Gaussian 09 software. By comparing  $[\text{EtOHmim}]^+ - \text{NH}_3$  system with  $[\text{Emim}]^+ - \text{NH}_3$  system, it can be found both the hydrogen bonding and interaction energy of  $[\text{EtOHmim}]^+ - \text{NH}_3$  system are stronger than those of  $[\text{Emim}]^+ - \text{NH}_3$  system. First, two representative structures of  $[\text{EtOHmim}]$  cation and  $\text{NH}_3$  have been calculated. One is  $\text{NH}_3$  located around  $\text{H}_{11}$  atom, the other is  $\text{NH}_3$  located around  $\text{H}_1$  atom. The optimized structures are shown in Figure 13 (a, b) and they are different from those in Shi's work<sup>27</sup>. It can be found that the hydrogen bonding is formed between N atom of  $\text{NH}_3$  and  $\text{H}_{11}$  with distance of 1.810 Å, and the relative interaction energy is  $-56.32 \text{ kJ mol}^{-1}$ . Similarly, the hydrogen bonding also can be formed between the N atom of  $\text{NH}_3$  and  $\text{H}_1$  with a distance of 2.131 Å, and the interaction energy is  $-47.42 \text{ kJ mol}^{-1}$ . The shorter bonding length and higher interaction energy show that  $\text{NH}_3$  prefers to interact with the  $\text{H}_{11}$  atom of hydroxyl than  $\text{H}_1$  atom for  $[\text{EtOHmim}]$  cation and  $\text{NH}_3$  system. For comparison, the same calculation method is used for  $[\text{Emim}]$  cation and  $\text{NH}_3$  system. The structures are shown in Figure 13 (c, d). The interaction energy between  $\text{NH}_3$  and  $[\text{Emim}]$  cation around  $\text{H}_1$  atom is  $-46.16 \text{ kJ mol}^{-1}$ , while that around  $\text{H}_1$  is only  $-20.98 \text{ kJ mol}^{-1}$ . What's more, the hydrogen bonding length between  $\text{H}_1$  and the N atom of  $\text{NH}_3$  (2.145 Å) is shorter than that between  $\text{H}_{11}$  and the N atom of  $\text{NH}_3$  (2.402 Å). The results show that  $\text{NH}_3$  is more inclined to interact with  $\text{H}_1$  atom of imidazole ring rather than  $\text{H}_{11}$  of  $\text{C}_2\text{H}_5$  group for  $[\text{Emim}]$  cation and  $\text{NH}_3$  system. By the comparison of the two systems, the higher  $\text{NH}_3$  absorption capacity of hydroxyl-functionalized ILs than that of conventional imidazolium ILs should be attributed to the strong hydrogen bonding and interaction energy.



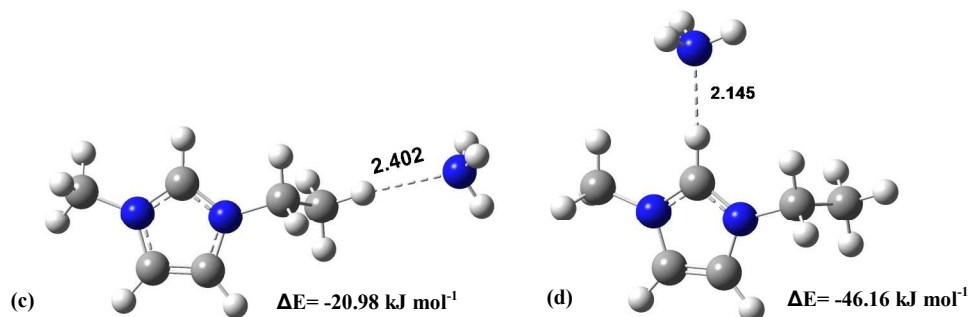


**Figure 13.** Optimized structures and interaction energies for [EtOHmim]<sup>+</sup>-NH<sub>3</sub> (a, b) and [Emim]<sup>+</sup>-NH<sub>3</sub> (c, d) systems. O, red; N, blue; H, white; N, gray. Hydrogen bonds are indicated by dotted lines, and distances are in angstroms.

#### 4. CONCLUSION

A series of hydroxyl-functionalized imidazolium ILs were synthesized and their physical properties as well as NH<sub>3</sub> absorption performance were systematically investigated. Compared with the conventional imidazolium ILs, the introducing of hydroxyl group results into the slight increase of viscosity, good thermal stability and improved NH<sub>3</sub> absorption capacity. Among these ILs, [EtOHmim][NTf<sub>2</sub>] has the highest NH<sub>3</sub> solubility, the mole fraction is 0.56 at 298.15 K and 159 kPa. The absorption cyclic experiments suggest these ILs can be regenerated. Furthermore, the absorption mechanism was detailedly studied by spectra analysis and quantum chemical calculations. The results demonstrate the excellent NH<sub>3</sub> absorption ability of these novel ILs is due to the strong hydrogen bonding between the N atom of NH<sub>3</sub> and the H atom of the hydroxyl on cation. Owing to the efficient absorption performance, simple preparation, good recyclability and excellent thermal stability, these hydroxyl-functionalized ILs could be promising candidates for NH<sub>3</sub> recovery.

#### ACKNOWLEDGEMENTS

The authors would like to acknowledge the National Basic Research Program of China (No. 2014CB744306), the National Natural Science Fund for Distinguished Young Scholars (No. 21425625), the Key Program of National Natural Science Foundation of China (21436010), and the Science and Technology Innovation Team of Cross and Cooperation of Chinese Academy of Sciences.

#### REFERENCES

1. J. W. Erisman, A. Bleeker, J. Galloway and M. S. Sutton, *Environmental pollution*, 2007, **150**, 140-149.
2. C. Maton, N. D. Vos and C. V. Stevens, *Chemical Society Reviews*, 2013, **42**, 5963-5977.



3. C. P. Fredlake, J. M. Crosthwaite, D. G. Hert, S. N. Aki and J. F. Brennecke, *Journal of Chemical & Engineering Data*, 2004, **49**, 954-964.
4. C. N. Dai, W. J. Wei, Z. G. Lei, C. X. Li and B. H. Chen, *Fluid Phase Equilibria*, 2015, **391**, 9-17.
5. H. S. Gao, S. J. Zeng, X. M. Liu, Y. Nie, X. P. Zhang and S. J. Zhang, *RSC Advances*, 2015, **5**, 30234-30238.
6. A. H. Jalili, M. Shokouhi, G. Maurer and M. Hosseini-Jenab, *Journal of Chemical Thermodynamics*, 2014, **74**, 286-286.
7. J. L. Anderson, K. D. Janeille and F. B. Joan, *Accounts of Chemical Research*, 2007, **40**, 1208-1216.
8. T. Nonthanasin, A. Henni and C. Saiwan, *RSC Advances*, 2014, **4**, 7566.
9. M. Ramdin, S. P. Balaji, J. Manuel Vicent-Luna, J. J. Gutierrez-Sevillano, S. Calero, T. W. de Loos and T. J. H. Vlugt, *Journal of Physical Chemistry C*, 2014, **118**, 23599-23604.
10. L. C. Tome, M. Isik, C. S. R. Freire, D. Mecerreyes and I. M. Marrucho, *Journal of Membrane Science*, 2015, **483**, 155-165.
11. Z. Z. Yang, Y. N. Zhao and L. N. He, *RSC Advances*, 2011, **1**, 545.
12. P. J. Carvalho and J. A. P. Coutinho, *Energy & Fuels*, 2010, **24**, 6662-6666.
13. G. K. Cui, W. J. Lin, F. Ding, X. Y. Luo, X. He, H. R. Li and C. M. Wang, *Green Chemistry*, 2014, **16**, 1211-1216.
14. G. K. Cui, C. M. Wang, J. J. Zheng, Y. Guo, X. Y. Luo and H. R. Li, *Chemical communications*, 2012, **48**, 2633-2635.
15. S. Y. Sun, Y. X. Niu, Q. Xu, Z. Sun and X. H. Wei, *RSC Advances*, 2015, **5**, 46564-46567.
16. Z. Z. Yang, L. N. He, Q. W. Song, K. H. Chen, A. H. Liu and X. M. Liu, *Physical chemistry chemical physics : PCCP*, 2012, **14**, 15832-15839.
17. S. J. Zeng, H. Y. He, H. S. Gao, X. P. Zhang, J. Wang, Y. Huang and S. J. Zhang, *RSC Advances*, 2015, **5**, 2470-2478.
18. S. J. Zeng, H. Y. He, H. S. Gao and X. P. Zhang, *RSC Advances*, 2015, **5**, 2470-2478.
19. Y. Zhao and G. X. Hu, *RSC Advances*, 2013, **3**, 2234-2240.
20. M. A. Ahmadi, R. Haghbakhsh, R. Soleimani and M. B. Bajestani, *Journal of Supercritical Fluids*, 2014, **92**, 60-69.
21. C. A. Faundez, J. F. Diaz-Valdes and J. O. Valderrama, *Fluid Phase Equilibria*, 2014, **375**, 152-160.
22. K. Huang, Y. L. Chen, X. M. Zhang, S. L. Ma, Y. T. Wu and X. B. Hu, *Fluid Phase Equilibria*, 2014, **378**, 21-33.
23. Y. Q. Ma and R. Wang, *Chemical Journal of Chinese Universities*, 2014, **35**, 1515-1522.
24. A. Yokozeki and B. S. Mark, *Industrial & Engineering Chemistry Research*, 2007, **46**, 1605-1610.
25. A. Yokozeki and M. B. Shiflett, *Applied Energy*, 2007, **84**, 1258-1273.
26. G. H. Li, Q. Zhou, X. P. Zhang, L. Wang, S. J. Zhang and J. W. Li, *Fluid Phase Equilibria*, 2010, **297**, 34-39.
27. W. Shi and E. J. Maginn, *AIChE Journal*, 2009, **55**, 2414-2421.
28. J. Palomar, G. Miquel-Maria, J. Bedia, F. Rodriguez and J. J. Rodriguez, *Separation and Purification Technology*, 2011, **82**, 43-52.
29. S. K. Tang, G. A. Baker and H. Zhao, *Chemical Society reviews*, 2012, **41**, 4030-4066.
30. J. Z. Zhang, C. Jia, H. F. Dong, J. Q. Wang, X. P. Zhang and S. J. Zhang, *Industrial & Engineering Chemistry Research*, 2013, **52**, 5835-5841.
31. M. Zhu, M. X. Zhu, Y. Song, W. Z. Liang, W. Han and Y. N. Chen, *Engineering and Manufacturing Technologies*, 2014, **541-542**, 78-82.
32. P. Brown, B. E. Gurkan and T. A. Hatton, *AIChE Journal*, 2015, **61**, 2280-2285.
33. L. J. Wazer JRV, Kim KY, Colwell RE, *New York: Wiley*, 1963, 406.
34. P. Navarro, M. Larriba, E. Rojo, J. Garcia and F. Rodriguez, *Journal of Chemical & Engineering Data*, 2013, **58**, 2187-2193.